

See discussions, stats, and author profiles for this publication at: <https://www.researchgate.net/publication/331574945>

# Grains, grain boundaries and total ionic conductivity of 10Sc1CeSZ and 8YSZ solid electrolytes affected by crystalline structure and dopant content

Article in *Materials today: proceedings* · January 2019

DOI: 10.1016/j.matpr.2018.10.078

CITATIONS

0

READS

35

8 authors, including:



**Iryna Brodnikovska**

National Academy of Sciences of Ukraine

10 PUBLICATIONS 6 CITATIONS

SEE PROFILE



**N.O. Korsunsk**

National Academy of Sciences of Ukraine

213 PUBLICATIONS 1,199 CITATIONS

SEE PROFILE



**L. Khomenkova**

V. Lashkaryov Institute of Semiconductor Physics, National academy of sci...

170 PUBLICATIONS 1,179 CITATIONS

SEE PROFILE



**Serhiy Lavoryk**

NanoMedTech, LLC, Kiev, Ukraine

28 PUBLICATIONS 89 CITATIONS

SEE PROFILE

Some of the authors of this publication are also working on these related projects:



ZrO<sub>2</sub>-based composites [View project](#)



High-k dielectrics doped with silicon and/or germanium for memory application [View project](#)



3<sup>rd</sup> ISE SSRSEU 2018

# Grains, grain boundaries and total ionic conductivity of 10Sc1CeSZ and 8YSZ solid electrolytes affected by crystalline structure and dopant content

I. Brodnikovska<sup>a\*</sup>, N. Korsunskaya<sup>b</sup>, L. Khomenkova<sup>b</sup>, Yu. Polishchuk<sup>b</sup>, S. Lavoryk<sup>b,c</sup>,  
M. Brychevskiy<sup>a</sup>, Y. Brodnikovskiy<sup>a</sup>, O. Vasylyev<sup>a</sup>

<sup>a</sup>Frantsevich Institute for Problems of Materials Science of National Academy of Sciences of Ukraine, 3 Krzhizhanovskoho St., 03680 Kyiv, Ukraine

<sup>b</sup>V. Lashkaryov Institute of Semiconductor Physics of the National Academy of Sciences of Ukraine, 45 Pr. Nauky, 03680 Kyiv, Ukraine  
<sup>c</sup>NanoMedTech LLC, 68 Antonovycha Str., 03680 Kyiv, Ukraine

---

## Abstract

Traditional 8YSZ and three types of promising 10Sc1CeSZ electrolytes made of commercial powders have been investigated due to their ionic conductivity. It has been shown that depending on the purity of the 10Sc1CeSZ powder and the chemical composition of its admixtures two types of preferable structure and electrical properties may be received. Evidences of Al<sup>3+</sup> and Sc<sup>3+</sup> in- and out diffusion between grain bulk and grain surface have been found. Both phenomena affect the grain boundary conductivity.

© 2018 Elsevier Ltd. All rights reserved.

Selection and peer-review under responsibility of the scientific committee of 3rd ISE Satellite Student Regional Symposium on Electrochemistry in Ukraine.

**Keywords:** 10Sc1CeSZ electrolytes; 8YSZ electrolytes; ionic conductivity; impedance spectroscopy; solid oxide fuel cells.

---

---

\* Corresponding author. Tel.: +3-8099-039-7703; fax: +3-8044-424-2131.

E-mail address: [Brodnikovska@i.ua](mailto:Brodnikovska@i.ua)

## 1. Introduction

Zirconium oxides with oxygen vacancies created by acceptor impurities are typical materials for solid oxide fuel cells (SOFC) electrolytes. These impurities stabilize  $ZrO_2$  in cubic phase, known for its high conductivity, and prevent phase transitions. Such dopants as  $Y_2O_3$ ,  $Sc_2O_3$  etc. are used to create oxygen vacancies [1]. As we consider zirconium electrolytes, 8 mol.% yttria-stabilized zirconia (8YSZ) is traditionally used, due to its good chemical and mechanical stability and affordable high quality of raw material [2]. Another promising zirconium electrolyte is 10 mol.% scandia-stabilized zirconia (10ScSZ), which has shown the highest ionic conductivity [3] due to the closure of the ionic radii of the  $Sc^{3+}$  dopant and the  $Zr^{4+}$  host ions, which leads to the low association of enthalpy between oxygen vacancies and  $Sc^{3+}$  doping ions. Small amounts of  $Ce_2O_3$  are added to 10ScSZ to prevent from unwanted phase transitions between rhombohedral and cubic phase at temperatures  $\sim 600$  °C [4], which results in an abrupt decrease of ionic conductivity [5], as well as diminishing electrical degradation of electrolytes, and, consequently, prolonging their lifetime [6].

The interfaces (boundaries or boundary complexions [7]) between grains and subgrains usually give the main contribution to the total ionic resistance of polycrystalline electrochemical materials. Two factors which affect mechanical and electrical properties of the material may be distinguished: dimensional factor (i.e. the influence of the particles size on total, grain and grain boundary conductivity of ceramics) and admixtures.

As we consider the first one, we have to notice that the value of electrical conductivity is in relation with Schottky barrier height, which depends on the vacancies density and admixtures segregation on the grains surface. The vacancies density correlates with the specific density of the grain boundaries in polycrystalline. While the grain size is increasing in submicron range, the specific density of the grain boundaries is decreasing causing the rise of admixtures segregations density. This leads to the increase of Schottky barrier height. When the grain size increases  $> 1$   $\mu m$ , the density of the admixture atoms on the grain surface reaches its critical value. After that they coagulate with the second phase particles creation. This decreases the concentration of admixture atoms on the grain surface, lowers the Schottky barrier height, and, therefore, enhances electrical conductivity. Thus, for  $ZrO_2$  co-doped with  $Sc_2O_3$  and  $CeO_2$  electrolyte it was shown [8] that bulk conductivity remains constant and grain boundary conductivity increases with the grain size increase in the range of 0.5-12  $\mu m$ . According to these explanations we can distinguish another opposite effect. For dense cubic YSZ ceramics with the grain size in submicron range (from 10 nm to 10  $\mu m$ ) it was shown [9] that the specific grain-boundary conductivity increases with decreasing grain size and bulk conductivity remains constant. Thus, we can see that although the size effect is a very important factor of grain boundary behavior, it is well predicted. But nanocrystallinity by itself does not guarantee exceptional transport properties of oxygen without a proper control of sample homogeneity and chemical purity.

This work deals rather with the chemical factor of grain and grain boundary conductivity as it is hardly to predict. The distribution of the main and admixture atoms in the electrolyte particles is determined by the synthesis method [10]. For example, it was shown [11, 12], that coprecipitation technique can allow Cu presence both in the crystallite volume and their surface simultaneously. The calcination temperature, in its turn, governs the redistribution of copper between the volume and the surface of the nanocrystals. Special attention should be paid to the effect of admixtures which influence the charge carriers transport and ionic conductivity of zirconium-based electrolytes due to the segregations on the grain surfaces.

The aim of our work was to compare the ionic conductivity of traditional 8YSZ and promising 10Sc1CeSZ solid electrolytes made of commercial powders, as well as to ascertain factors affecting the value of conductivity and activation energy of ceramics obtained under certain technological conditions.

## 2. Materials and methods

10Sc1CeSZ ceramic electrolytes were obtained from 10 mol%  $Sc_2O_3$  – 1 mol%  $CeO_2$  – 89 mol%  $ZrO_2$  powders of three types: 1) VMMC (Ukraine), obtained by co-precipitation; 2) DKKK (Japan), obtained by hydrothermal synthesis and 3) Praxair (USA) obtained by spray-pyrolysis. According to the type of initial powder, the samples were named 10Sc1CeSZ-1, 10Sc1CeSZ-2 and 10Sc1CeSZ-3. 8YSZ samples were obtained from 8 mol.%  $Y_2O_3$  – 92 mol.%  $ZrO_2$  (Tosoh, Japan). Some structural, mechanical properties as well as the results of the comparative analysis of all three types of 10Sc1CeSZ powders were described in details earlier [10, 13] (Tables 1 and 2).

Powders were milled with zirconia balls in a medium of ethyl alcohol for 24 hours and dried in air. Samples were pre-pressed under 30 MPa into the discs of 15 mm × 1.5-2 mm and then sintered at 1250-1550 °C in air. 10Sc1CeSZ and 8YSZ electrolytes sintered at 1400 °C were chosen for impedance spectroscopy investigations due to the best values of conductivity at 600 °C, according to our earlier studies [14].

Table 1. Characteristics of 10Sc1CeSZ powders [10].

Powder	Particle size† (nm)	Average size of agglomerates (μm)	Specific surface area (m <sup>2</sup> /g)
10Sc1CeSZ-1	20-50	2.4	50
10Sc1CeSZ-2	100-200	0.1-1	11.6
10Sc1CeSZ-3	100-300	18	4.6

Table 2. Bulk chemical composition of electrolyte samples [10].

Sample	Chemical composition‡ (wt.%)									
	Sc	Ce	Si	Fe	Al	Ti	Ca	Mg	Na	K
10Sc1CeSZ-1	10.1	0.94	<0.1	0.01	0.025	0.01	0.01	0.02	0.008	0.003
10Sc1CeSZ-2	10.1	1.16	<0.004	0.004	<0.002	0.001	0.001	-	0.0024	-
10Sc1CeSZ-3	10.2	1.02	0.049	0.01	0.005	0.14	<0.01	>0.01	0.002	0.0007

Structural properties were studied by x-ray diffraction (XRD) method. XRD data were collected in the range of  $2\Theta = 20\text{--}80^\circ$  using Thermo Scientific ARL X'TRA diffractometer with Cu K $\alpha$  radiation ( $\lambda = 0.15418$  nm) in Bragg geometry.

Diffuse reflectance (DR) spectra were recorded with respect to the BaSO<sub>4</sub> standard at room temperature by means of double-beam spectrophotometer UV-3600 UV-VIS NIR (Shimadzu Company) equipped with an integrated sphere ISR-3100. Obtained spectra were transformed in absorption ones using standard program based on the Kubelka-Munk ratio  $f(r_\infty) = (1 - r_\infty)^2 / 2r_\infty = K/S$ , where  $f(r_\infty)$  is the Kubelka-Munk function,  $r_\infty = R_{\text{sample}} / R_{\text{BaSO}_4}$  is the relative diffuse reflection from the sample,  $K$  and  $S$  are absorption and scattering coefficients of the sample, respectively. Some structural investigations (XRD, diffused reflectance spectra) were performed on initial and calcined at 700, 800 and 900 °C 10Sc1CeSZ powders as well.

The surface/bulk composition of samples was characterized by Secondary Ions Mass Spectrometry (SIMS) using argon ion beam (3 keV, current density 5 μA/cm<sup>2</sup>) for sputtering and MC-7201 monopole mass spectrometer for detection of the secondary ions.

Impedance spectroscopy investigations were provided at temperatures of 400-800 °C for 10Sc1CeSZ and 200-700 °C for 8YSZ in the frequency range of 10<sup>-2</sup>-10<sup>6</sup> Hz using Solartron 1260 Impedance/Gain-Phase Analyzer. For the formation of electrodes, a silver paste was applied to the surface of the samples and burned off under appropriate conditions. Impedance spectra were modeled by means of two parallel equivalent  $R$ - $CPE$  circuits connected in series. Low frequency semicircle was attributed to the charge relaxation on the grain boundaries, high frequency semicircle – to the relaxation of vacancies inside the grains. Parameters of the model gave information about resistive and capacitive properties of grain and grain boundary. The samples of stabilized zirconia had a significant difference in porosity depending on the type of initial powder (10Sc1CeSZ-1 – 32%, 10Sc1CeSZ-2 – 2%, 10Sc1CeSZ-3 – 17% [13, 14], 8YSZ – 2%).

† By XRD-TEM data.

‡ As related to oxide forms.

### 3. Results and discussion

#### 3.1. XRD data

As we can see from Fig. 1b-c, four characteristic XRD reflections at  $2\Theta \approx 30.3^\circ$ ,  $35.2^\circ$ ,  $50.6^\circ$  and  $74.5^\circ$  testify to cubic crystalline structure in all 10Sc1CeSZ powders regardless of their type. Calcination temperature does not shift the peaks or change their intensity. As far as most of the peaks which belong to tetragonal and cubic phases are close to each other [11], additional examination was used to discriminate unambiguously these phases. In the range of  $2\Theta = 73-75^\circ$  cubic phase shows only a single peak at  $2\Theta \approx 74.5^\circ$  for initial and calcined at 700-900 °C 10Sc1CeSZ powders, while the tetragonal phase should demonstrate two peaks at  $2\Theta \approx 73^\circ$  and  $74.6^\circ$ . Thus, we can conclude that no cubic-tetragonal phase transitions appear in scandia-stabilized zirconia doped with ceria at  $\sim 600^\circ\text{C}$  as it may happen without  $\text{Ce}_2\text{O}_3$  additive [4].

Yttria-stabilized zirconia shows characteristic reflection peaks at  $30.1^\circ$ ,  $34.9^\circ$ ,  $50.2^\circ$  (Fig. 1a). Close examination of reflection peaks at  $2\Theta = 73-75^\circ$  shows one characteristic peak at  $73.7^\circ$  which is the feature of a cubic structure.

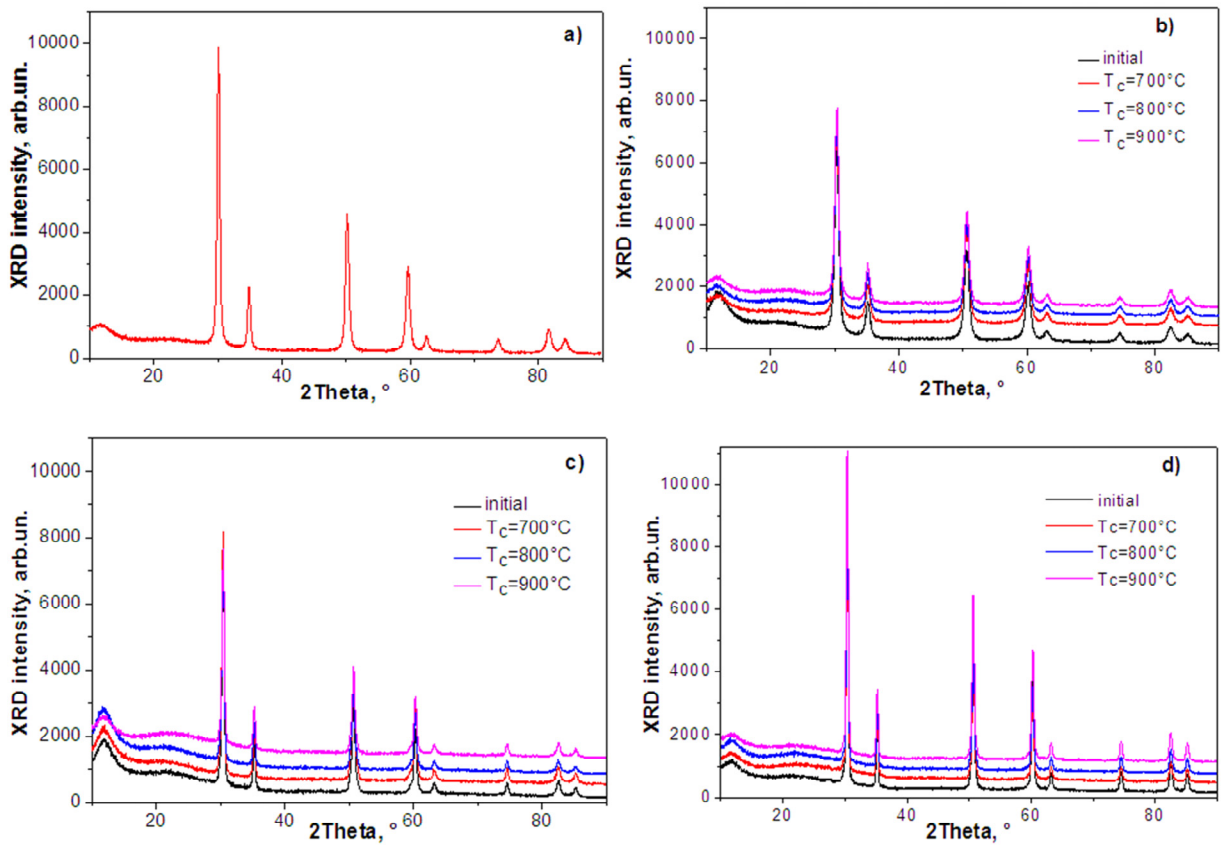


Fig. 1. XRD patterns of initial and calcined at 700-900 °C (a) 8YSZ, (b) 10Sc1CeSZ-1, (c) 10Sc1CeSZ-2 and (d) 10Sc1CeSZ-3 powders.

#### 3.2. Diffuse reflectance spectra

Figure 2a shows diffuse reflectance spectra of initial 10Sc1CeSZ and 8YSZ powders, Fig. 2b and 2c – DR spectra of initial powders, calcined powders and sintered electrolytes of type 1 and type 2 respectively, Fig. 2d - DR spectra of initial and calcined type 3 powders. As previous  $\text{ZrO}_2$  study showed [12], these DR spectra contain the absorption band (peaked at  $\sim 270\text{ nm}$ ) near the band edge of  $\text{ZrO}_2$ . According to this study, this band is assumed to be caused by oxygen vacancies in the nanocrystals.

The intensity of the peaks of initial powders (Fig. 2a) increases from 8YSZ to 10Sc1CeSZ-2, 10Sc1CeSZ-3 and 10Sc1CeSZ-1, being accompanied by the shift of their peak position.

The initial powder of type 1 demonstrates the highest absorption at about 270 nm (Fig.2b). Calcined powders demonstrate the decrease of DR intensity without the peak shifts. Being sintered, the intensity of absorption band decreases with temperature increase from 1250 to 1550 °C, one peak (at ~270 nm) turns to two (~270 and ~330 nm) collocated peaks. For powders of type 2 (Fig.2,c) similar behavior of DR spectra is found. When sintered at 1275-1300 °C electrolytes demonstrate the peak shift to 275 nm, and to 300 nm when sintered at 1300-1450 °C. The powder of the first type is enriched by Si and Al impurities (Table 2). Impurity atoms of  $Al^{3+}$  with small atomic radius can penetrate to the electrolyte grains and even create oxygen vacancies. Therefore, they can also contribute to absorption band at ~270 nm, as it was shown for Cu [12]. Thus, we can assume, that the significant decrease of absorption intensity at  $T_c=900$  °C may be related to the outward diffusion of  $Al^{3+}$  from the grain bulk to the grains surface and consequent formation of mullite along the boundaries in reaction with silica. The phenomenon of the peak shift may be related to the change of the bonds between vacancies and doping cations. Even being associated to impurity atoms, oxygen vacancies steel can contribute to the absorption.

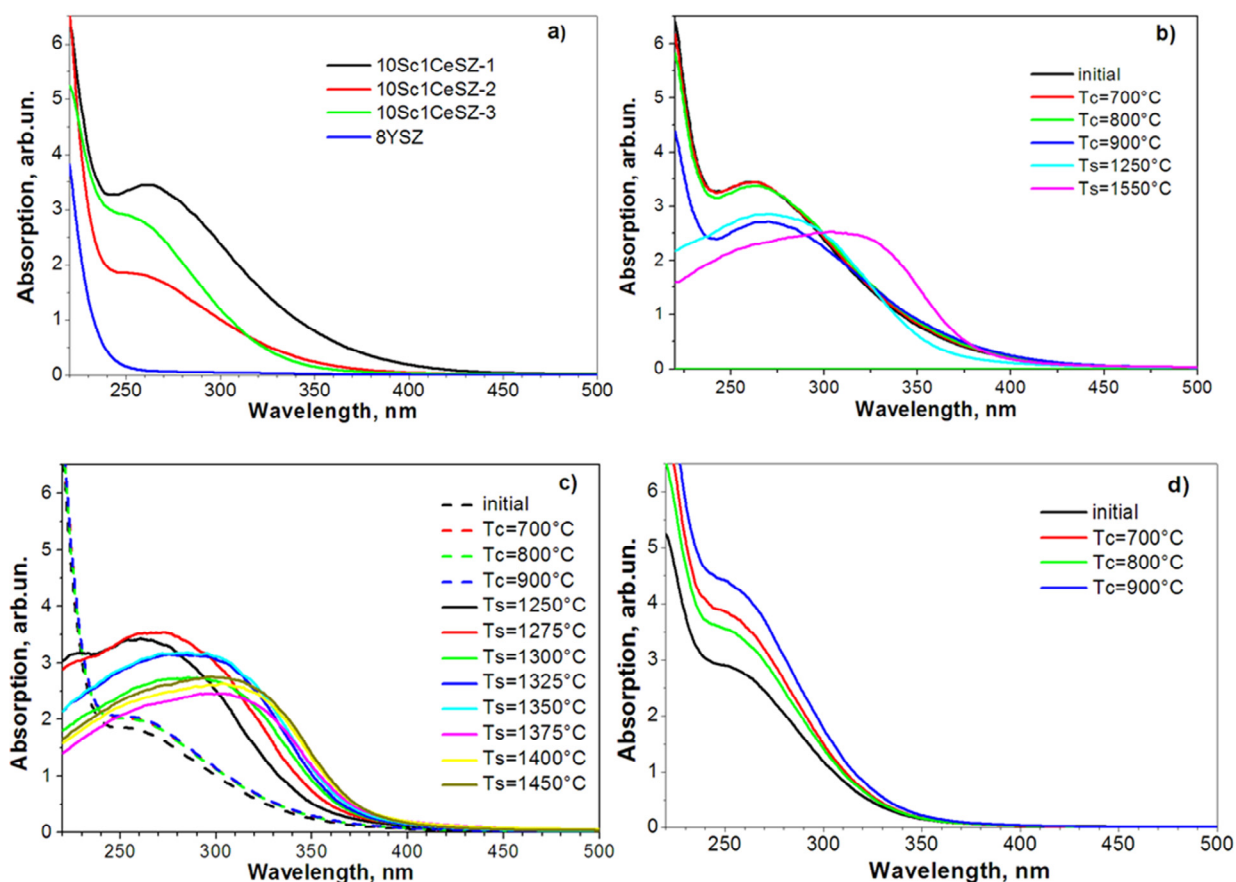


Fig. 2. Diffuse reflectance spectra of initial, calcined ( $T_c=700-900$  °C) and sintered ( $T_s=1250-1450$  °C) (a) 8YSZ, (b) 10Sc1CeSZ-1, (c) 10Sc1CeSZ-2, (d) 10Sc1CeSZ-3 powders and electrolytes.

For 10Sc1CeSZ-2 powders the position of peak intensity fluctuates around 270 nm with a slight increase with increasing calcination temperature (Fig. 2c). It rises sharply to 285-290 nm when electrolytes are sintered at 1250-1275 °C. At higher  $T_s$ , the intensity decrease is accompanied by the appearance of two peaks around 270 and 300 nm.

The peak position of 10Sc1CeSZ-3 powder absorption is about 250 nm and it does not change with calcination temperature. The absorption intensity increases with increase of calcination temperature. It is known from our previous investigations [10] that the difference between 10Sc1CeSZ-3 powders and the others is that: 1) their surface layer is enriched by  $\text{Sc}^{3+}$  more than two times in comparison with bulk; 2) titanium prevails in chemical composition of impurities. As titanium has large cations and they cannot incorporate into grains, the absorption intensity increase may be due to the incorporation of  $\text{Sc}^{3+}$  into the grains and additional creation of oxygen vacancies. Unfortunately, diffuse reflectance spectra of 10Sc1CeSZ-3 ceramics were not recorded.

### 3.3. Impedance spectroscopy

As we can see from Fig. 3a, grain boundary conductivity of 8YSZ electrolytes is higher than grain conductivity. Thus, ionic conductivity of 8YSZ electrolytes occurs mainly through the grain boundaries. The crystalline structure of yttria-stabilized samples was cubic (Fig. 1a), which has the highest conductivity compared to tetragonal and monoclinic zirconia. No traces of phase transitions which could negatively affect the conductivity were found. A low absorption at 270 nm (Fig. 2a) shows lower amount of oxygen vacancies in the grains in 8YSZ compared to the 10Sc1CeSZ powders, which may be due to lower dopant content in YSZ powders.

The activation energy of 8YSZ grain is higher than that for grain boundary phase – 1.16 eV and 1.12 eV respectively. Activation energy of total conductivity of 8YSZ electrolytes is 1.04 eV in the temperature range of 263–556 °C and it drops to 0.57 eV at 601–685 °C. According to [15], the association (the dopant-vacancy clusters  $Y'_zV_o^{II}$ ) predominates in YSZ grains below 560 °C. Due to the field effect and the depletion of oxygen vacancies, the association should be negligible near the grain boundaries, i. e., the defects near the boundaries are mainly free at temperatures <560 °C [16]. Thus, we can assume that an extremely low oxygen vacancies content and their association with  $Y^{3+}$  dopants inside the grains make the charge carriers move predominantly along the grain boundaries which are bad conductors themselves.

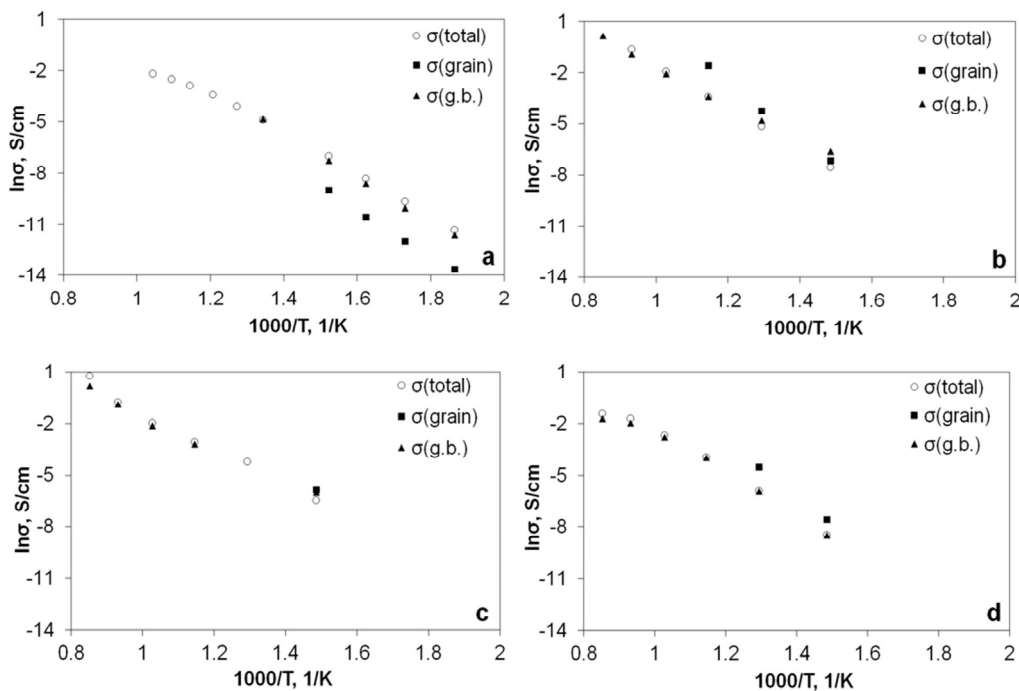


Fig. 3. Temperature dependence of grain, grain boundary and total ionic conductivity of (a) 8YSZ, (b) 10Sc1CeSZ-1, (c) 10Sc1CeSZ-2 and (d) 10Sc1CeSZ-3 electrolytes.

Chemically pure 10Sc1CeSZ-2 electrolytes had the highest total ionic conductivity (0.046 S/cm at 600 °C) due to close to zero grain resistance (Fig. 3c). Total ionic conductivity of the type 1 electrolytes is high enough (0.033 S/cm

at 600 °C) (Fig. 3b) but its value could be higher if ceramics has higher density. Total ionic conductivity of 10Sc1CeSZ-3 electrolytes was the lowest between scandia-ceria-stabilized samples – 0.019 S/cm at 600 °C (Fig. 3d). Despite these electrolytes have density much higher than that for the type 1 electrolytes, their grain boundary conductivity is lower twice (0.018 S/cm and 0.033 S/cm at 600 °C respectively). As diffused reflectance spectra of these powders (Fig. 2a, b, d) showed that fundamental absorption in initial 10Sc1CeSZ-1 powders first prevails, and after calcination at 900 °C the tendency is opposite, we can assume that the reason of such difference in grain boundary conductivities of these two electrolytes is the relative composition of impurities. When  $\text{Al}^{3+}$  undergoes outward diffusion from the grain bulk to the grains surface in 10Sc1CeSZ-1 electrolytes, it reacts with silica (known for its reducing the grain boundary conductivity) and gives a mullite. Such effect of small amount of alumina addition (up to 0.5 wt.%) is known as “scavenging effect” [17]. The concept of properties improving by means of admixtures may be called “the concept of useful and non-useful admixtures” and it was discovered and reported by Arkharov long ago [18].

When compare DR spectra with ionic conductivity of materials obtained at different sintering temperatures [14] we have to notice that the highest ionic conductivity correlates with the highest area under absorption band. Thus, to identify the absorption peaks and to assign them to associated or free oxygen vacancies will be the next step of our investigations.

#### 4. Conclusions

1. Three types of 10Sc1CeSZ solid electrolytes have been obtained. The highest values of ionic conductivity can be obtained due to: 1) using of highly chemically pure initial powders. In this case high ionic conductivity (0.046 S/cm at 600 °C) is reached due to close to zero grain resistance; 2) using of “the concept of useful and non-useful admixtures” in technically pure initial powders. Favorable chemical composition of admixtures can lower grain boundary resistance twice and increase total ionic conductivity to 0.033 S/cm at 600 °C even at high porosity of 32%.

2. Outward diffusion of  $\text{Al}^{3+}$  from the grain bulk to the grains surface and consequent formation of mullite along the boundaries in reaction with silica has been assumed in 10Sc1CeSZ-1 electrolytes due to the excess of Al in chemical composition of the initial powders. This phenomenon lowered grain boundary resistance twice.

3. The incorporation of  $\text{Sc}^{3+}$  and additional creation of oxygen vacancies in the grains have been assumed in 10Sc1CeSZ-3 electrolytes.

#### References

- [1] S. Kazlauskas, E. Kazakevičius, A. Kežionis, *Solid State Ionics* 310 (2017) 143–147.
- [2] E. Ivers-Tiffée, A. Weber, D. Herbstritt, *J. Eur. Ceram. Soc.* 21 (2001) 1805–1811.
- [3] M. Liu, C.R. He, W.G. Wang et al., *Ceram. International* 40(4) (2014) 5441–5446.
- [4] S. Omar, *Solid State Ionics* 184(1) (2010) 2–5.
- [5] Y. Arachi, T. Asai, O. Yamamoto et al., *J. Electrochem. Soc.* 148 (5) (2001) A520–A523.
- [6] S. Omar, W.B. Najib, N. Bonanos, *Solid State Ionics* 189 (2011) 100–106.
- [7] P.R. Cantwell, M. Tang, S.J. Dillon et al., *Acta Mater.* 62 (2014) 1–48.
- [8] D.S. Lee, W.S. Kim, S.H. Choi et al., *Solid State Ionics* 176 (2005) 33–39.
- [9] I. Kosacki, H.U. Anderson, *Encyclopedia of Materials: Science and Technology*, Elsevier Science Ltd., New York, 2001, vol.4, pp. 3609 - 3617.
- [10] A. Smirnova, V. Sadykov, V. Muzykantov et al., *Mater. Res. Soc. Symp. Proc. Vol. 972 (2006) 0972-AA10-05*.
- [11] N. Korsunskaya, Yu. Polishchuk, V. Kladko et al., *Mater. Res. Express* 4 (2017) 035024.
- [12] N. Korsunskaya, M. Baran, I. Vorona et al., *Nanoscale Research Letters* (2017) 12:157.
- [13] O.D. Vasylyev, A.L. Smirnova, M.M. Brychevskiy et al., *Material Science of Nanostructures* 1 (2011) 70–80.
- [14] O. Vasylyev, M. Brychevskiy, Y. Brodnikovskiy et al., *Electronic Microscopy and Strengths of Materials*, Frantsevich Institute for Problems of Materials Science of NASU, Kyiv, 2015, vol. 21, pp. 86–101.
- [15] M. Filal, C. Petot, M. Mokchah et al., *Solid State Ionics* 80 (1995) 27–35.
- [16] X. Guo, R. Waser, *Prog. Mater. Sci.* 51 (2006) 151–210.
- [17] C.X. Guo, J.X. Wang, C.R. He et al., *Ceram. Intl.* 39 (2013) 9575–9582.
- [18] V. Arkharov, *The Oxidation of Metals at High Temperatures*, Metallurgizdat, Sverdlovsk, 1945, 171 p., in Russian.